Available online at www.sciencedirect.com
ScienceDirect
Journal of Solid State Chemistry 179 (2006) 3926–3936
JOURNAL OF SOLID STATE CHEMISTRY
www.elsevier.com/locate/jssc

Metal dicyanamide layered coordination polymers with cyanopyridine co-ligands: Synthesis, crystal structures and magnetism

Miao Du[a,*], Qian Wang[a], Ying Wang[a], Xiao-Jun Zhao[a], Joan Ribas[b]

[a]*College of Chemistry and Life Science, Tianjin Normal University, Tianjin 300074, PR China*
[b]*Departament de Química Inorgànica, Universitat de Barcelona, Diagonal, 647, 08028-Barcelona, Spain*

Received 6 July 2006; received in revised form 23 August 2006; accepted 26 August 2006
Available online 15 September 2006

Abstract

A series of metal dicyanamide (dca) coordination polymers combined with cyanopyridine (cypy) terminal co-ligands, namely, $[Co_2(dca)_4(4\text{-cypy})_4]_n$ (**1**), $[Cd(dca)_2(4\text{-cypy})_2]_n$ (**2**), $[Fe(dca)_2(3\text{-cypy})_2]_n$ (**3**) and $[Co(dca)_2(3\text{-cypy})_2]_n$ (**4**), have been synthesized at the ambient conditions. X-ray single crystal diffraction reveals that complexes **1**–**4** have similar metal-dca coordination layers in which the octahedral metal centers are connected by $\mu_{1,5}$-dca linkers. Notably, three types of 3-D packing lattices are observed for these layered arrays. The thermal stabilities of such new crystalline materials have been studied by thermogravimetric analysis of mass loss. The magnetic properties of the Co^{II} and Fe^{II} complexes have been investigated and discussed in detail. A discrete mononuclear molecule $[Cd(dca)_2(pyom)_2]$ (**5**) is also described, in which the chelated ligand *O*-methyl picolinimidate (pyom) arises from the addition of methanol solvent across the C≡N bond of 2-cypy.

Keywords: Metal dicyanamide; Auxiliary ligand; Layered complex; Crystal structure; Magnetochemistry

1. Introduction

Crystal engineering of coordination polymers [1] based on pseudohalide ligands such as dicyanamide [dca, $N(CN)_2^-$] has been recently of considerable interest, especially the early reports of a series of binary $[M(dca)_2]_n$ complexes that exhibit the 3-D rutile network topology and intriguing long-range magnetic ordering [2]. Surely, it is a significant research to utilize the anionic dca bridge together with other auxiliary organic co-ligands to construct new coordination architectures that behave a variety of network topologies from 1-D to 3-D as well as different magnetic properties [3,4]. Remarkably, the structural diversity of such supramolecular systems is primarily ascribed to the coordination versatility of the dca anion, which is testified to show as many as eight possible binding modes using its nitrile and/or amide nitrogen with metal ions under different surroundings [3].

With regard to the organic co-ligands, they can be classified as two types according to their distinct coordinated characters. The bridging ones such as the typical linkers pyrazine and 4,4′-dipyridyl may further extend the metal-dca coordination arrays to produce new crystalline materials [3,4b,4d,5]. Although the terminal ligands seem only to complete the coordination sphere of a given metal ion, in fact, they also have somewhat impacts on the final metal-dca binding networks [3,6]. For example, a single dca-bridged chain is found for $[Mn(dca)_2(2,2'\text{-biimidazole})]_n$ [4c], whereas a series of double dca-connected 1-D architectures are generated with the replacement of the co-ligand by 4-picoline [4c], pyridine [7a], 4-benzoylpyridine [7b], 2,2′-bipyridine [7b,7c] or 2-aminopyrimidine [7d]. Meantime, a 1-D tubelike coordination motif is observed for $\{[Mn(dca)_2(4,4'\text{-dipyridyl})(H_2O)]\cdot 0.5H_2O\}_n$ [7c], in which the 4,4′-dipyridyl is monodentate. Moreover, 2-D layered Mn-dca coordination polymers could be achieved when 4-cyanopyridine [7e] or chelated 1,10-phenanthroline [6a] is applied. Similar cases are also detected in the Cu^{II} complexes of dicyanamide with different terminal co-ligands [8]. Notably, a 3-D bimetallic coordinated network

*Corresponding author. Fax: +86 22 23540315.
E-mail address: dumiao@public.tpt.tj.cn (M. Du).

0022-4596/$ - see front matter © 2006 Elsevier Inc. All rights reserved.
doi:10.1016/j.jssc.2006.08.039

$\{[Cu(pn)_2][Mn(dca)_4]\}_n$ (pn = 1,3-diaminopropane) with a 3-fold interpenetrating diamond topology is presented [9]. Of further interest, in all above examples dca adopts the most common $\mu_{1,5}$ binding fashion.

Recently, we have introduced n-cyanopyridine ligands ($n = 2-4$, cypy) into the Cu^{II}–dca systems to produce a series of 1-D single or double dca-bridged chain complexes [10]. Although such ligands contain two types of nitrogen donors, they usually use only pyridyl to participate the metal coordination due to its stronger donor inherence [11]. Notably, the free cyano moiety prefers to be involved in the weak C–H···N interactions, interlinking the 1-D structures to form 3-D interpenetrating networks [10]. As an extension of this research, our current work has focused on related ternary systems with other transition metal ions. In this context, four layered coordination polymers via dca connectors $[Co_2(dca)_4(4\text{-cypy})_4]_n$ (**1**), $[Cd(dca)_2(4\text{-cypy})_2]_n$ (**2**), $[Fe(dca)_2(3\text{-cypy})_2]_n$ (**3**) and $[Co(dca)_2(3\text{-cypy})_2]_n$ (**4**) have been prepared and structurally determined by X-ray single crystal diffraction. The magnetic properties of the 2-D Co^{II} and Fe^{II} materials have also been analyzed in detail. As for 2-cypy, the in situ generation of a chelated ligand *O*-methyl picolinimidate (pyom) is found when it reacts with Cd^{II} and dca, which leads to the formation of a discrete monomeric complex $[Cd(dca)_2(pyom)_2]$ (**5**).

2. Experimental

2.1. Materials and general methods

All the starting materials for synthesis and analysis were commercially available and used as received. Fourier transform (FT) IR spectra (KBr pellets) were taken on an AVATAR-370 (Nicolet) spectrometer. Carbon, hydrogen, and nitrogen analyses were performed on a CE-440 (Leemanlabs) analyzer. Thermogravimetric analysis (TGA) experiments were carried out on a Dupont thermal analyzer from room temperature to 800 °C under nitrogen atmosphere at a heating rate of 10 °C/min.

2.2. Magnetic studies

Magnetic measurements were performed in the "Servei de Magnetoquímica (Universitat de Barcelona)" on polycrystalline samples (30 mg) with a Quantum Design SQUID MPMS-XL susceptometer, working in the temperature range of 2–300 K. The magnetic field was changed from 50 to 10,000 G. The diamagnetic corrections were evaluated from Pascal's constants for all constituent atoms.

2.3. Syntheses of complexes 1–5

2.3.1. $[Co_2(dca)_4(4\text{-cypy})_4]_n$ (1)

4-Cypy (10.4 mg, 0.1 mmol) and Na(dca) (36.0 mg, 0.4 mmol) were dissolved in a CH_3CN/CH_3OH solution (v: v = 1: 1, 15 ml). The mixture was stirred and heated for 5 min. Then a water solution (5 ml) of $CoCl_2 \cdot 6H_2O$ (47.4 mg, 0.2 mmol) was added. The resultant light red solution was filtered off and left to stand at room temperature. Red block crystals suitable for X-ray diffraction were obtained within 1 week in a 66% yield (13.2 mg, based on 4-cypy). Anal. Calcd for $C_{32}H_{16}Co_2N_{20}$ (798.51): C, 48.14; H, 2.02; N, 35.08. Found: C, 47.63; H, 2.20; N, 35.41. IR (cm^{-1}): 3101 w, 2310 s, 2255 s, 2188 vs, 1609 s, 1550 m, 1498 w, 1415 s, 1370 s, 1219 m, 1070 w, 1018 w, 832 s, 776 w, 669 w, 562 s, 515 m.

2.3.2. $[Cd(dca)_2(4\text{-cypy})_2]_n$ (2)

The same synthetic method as that for **1** was used except that $CoCl_2$ was replaced by $Cd(NO_3)_2 \cdot 4H_2O$ (61.6 mg, 0.2 mmol), generating colorless lamellar crystals after 3 days in a 71% yield (16.1 mg, based on 4-cypy). Anal. Calcd for $C_{16}H_8CdN_{10}$ (452.72): C, 42.45; H, 1.78; N, 30.94. Found: C, 41.99; H, 1.55; N, 30.65. IR (cm^{-1}): 3093 w, 2306 s, 2248 m, 2175 vs, 1602 m, 1544 w, 1496 w, 1417 m, 1360 s, 1215 w, 1066 w, 1010 m, 832 m, 783 w, 666 w, 561 m, 517 m.

2.3.3. $[Fe(dca)_2(3\text{-cypy})_2]_n$ (3)

The same synthetic method as that for **1** was used except that $CoCl_2$ and 4-cypy was replaced by $Fe(ClO_4)_2 \cdot 6H_2O$ (36.0 mg, 0.1 mmol) and 3-cypy (10.5 mg, 0.1 mmol), respectively, producing yellow block crystals after 3 weeks in a 15% yield (3.0 mg, based on 3-cypy). A quantitative synthesis of the bulk microcrystalline sample of **3** could be achieved by direct mixing of the starting reagents dissolved in a small amount of solvents, the phase purity of which was identified by powder X-ray diffraction. Anal. Calcd for $C_{16}H_8FeN_{10}$ (396.17): C, 48.51; H, 2.04; N, 35.36. Found: C, 48.80; H, 1.91; N, 35.32. IR (cm^{-1}): 3062 w, 2297 s, 2239 m, 2170 vs, 1594 m, 1474 m, 1417 m, 1357 s, 1189 w, 1047 w, 936 w, 822 m, 696 m, 667 w, 646 w, 522 m.

2.3.4. $[Co(dca)_2(3\text{-cypy})_2]_n$ (4)

The same synthetic method as that for **3** was used except that $Fe(ClO_4)_2 \cdot 6H_2O$ was replaced by $Co(Ac)_2 \cdot 4H_2O$ (50 mg, 0.2 mmol), giving light-red block crystals after 2 weeks in a 72% yield (14.4 mg, based on 3-cypy). Anal. Calcd for $C_{16}H_8CoN_{10}$ (399.25): C, 48.14; H, 2.02; N, 35.08. Found: C, 47.46; H, 1.82; N, 34.58. IR (cm^{-1}): 3062 w, 2297 s, 2242 m, 2174 vs, 1596 m, 1474 m, 1418 m, 1356 s, 1189 w, 1130 w, 1048 w, 935 w, 822 m, 696 m, 668 w, 647 w, 519 m.

2.3.5. $[Cd(dca)_2(pyom)_2]$ (5)

The same synthetic method as that for **2** was used except that 4-cypy was replaced by 2-cypy (10.4 mg, 0.1 mmol), affording colorless lamellar crystals after 4 days in a 75% yield (19.3 mg, based on 2-cypy). Anal. Calad for $C_{18}H_{16}CdN_{10}O_2$ (516.81): C, 41.83; H, 3.12; N, 27.10. Found: C, 41.46; H, 2.83; N, 26.64. IR (cm^{-1}): 3248 m, 3034 w, 2274 s, 2220 s, 2158 vs, 1653 s, 1590 s, 1483 w,

1435 m, 1373 s, 1298 w, 1265 w, 1188 m, 1136 s, 1099 w, 1051 w, 1012 m, 968 w, 876 m, 805 m, 752 m, 691 m, 672 w, 637 w, 511 m.

Caution! Metal perchlorate complexes in the presence of organic ligands are potentially explosive. Only a small amount of material should be handled with care.

2.4. X-ray crystallography

Single-crystal X-ray diffraction data for complexes **1**–**5** were collected on a Bruker Apex II CCD diffractometer at 293(2) K with Mo Kα radiation ($\lambda = 0.71073$ Å). There was no evidence of crystal decay during data collection for all cases. A semiempirical absorption correction was applied using SADABS, and the program SAINT was used for integration of the diffraction profiles [12a]. The structures were solved by direct methods using SHELXS and refined by full-matrix least squares on F^2 with SHELXL [12b]. Hydrogen atoms attached to carbon were placed geometrically and allowed to ride during the subsequent refinement. For **5**, starting positions of the imine H atoms were located in difference Fourier syntheses, and then positioned geometrically and treated as the riding atoms. One of the 4-cypy molecules in **1** was treated using a disordered model, which was divided into two equivalent parts. Further crystallographic data and structural refinement parameters are summarized in Table 1.

3. Results and discussion

3.1. Preparation and general characterization of the complexes

Solution assemblies of cypy and Na(dca) with different metal salts produce layered complexes **1**–**4**, which are air stable and insoluble in common organic solvents (such as acetone, THF, DMF, CH_3OH, C_2H_5OH, CH_3CN, CH_2Cl_2 and $CHCl_3$) and water. For the discrete molecule of compound **5**, it is subtly soluble in DMF and CH_3OH. In the formation of **5**, the C≡N group of 2-cypy suffers a nucleophilic addition by CH_3OH solvent to give the ligand *O*-methyl picolinimidate (pyom), being similar to the case of Cu^{II} [10].

In the IR spectra of **1**–**5**, the absorption peaks in 1400–1600 cm^{-1} are attributed to the skeletal vibrations of the pyridyl group of the ligands. For **1**–**4**, the characteristic bands of dca anion are similar, and shift significantly toward the higher frequencies compared with those of Na(dca) and **5**, indicating a bridging coordination mode [10]. This is also consistent with the results of the structural analysis as described below. Additionally, there is a very sharp band with medium intensity at 3248 cm^{-1} for **5**, being due to the N−H stretching of the imine moiety of pyom.

The thermal stabilities of **1**–**4** were studied by thermogravimetric analysis (TGA) experiments. In the TGA curve of **1**, the first sharp weight loss of 52.62% in 146–231 °C

Table 1
Crystallographic data and structure refinement summary for complexes **1**–**5**

	1	**2**	**3**	**4**	**5**
Empirical formula	$C_{32}H_{16}Co_2N_{20}$	$C_{16}H_8CdN_{10}$	$C_{16}H_8FeN_{10}$	$C_{16}H_8CoN_{10}$	$C_{18}H_{16}CdN_{10}O_2$
Mr	798.51	452.72	396.17	399.25	516.81
Crystal size (mm)	0.30 × 0.26 × 0.20	0.45 × 0.13 × 0.04	0.20 × 0.18 × 0.16	0.21 × 0.15 × 0.10	0.26 × 0.13 × 0.05
Crystal habit	Red block	Colorless lamellar	Yellow block	Light-red block	Colorless lamellar
Crystal system	Monoclinic	Orthorhombic	Monoclinic	Monoclinic	Monoclinic
Space group	*Pc*	*Pccn*	*C*2/*c*	*C*2/*c*	$P2_1/c$
a (Å)	7.982(3)	9.5135(9)	14.547(7)	14.504(3)	8.835(3)
b (Å)	18.776(7)	12.4374(12)	8.957(4)	8.9191(16)	15.002(5)
c (Å)	12.482(5)	14.4942(13)	13.859(7)	13.749(2)	16.813(6)
β (°)	91.004(7)	90	112.609(7)	112.446(2)	105.175(4)
V (Å^3)	1870.3(13)	1715.0(3)	1667.1(14)	1643.9(5)	2150.9(12)
Z	2	4	4	4	4
D_c (g cm^{-3})	1.418	1.753	1.578	1.613	1.596
μ (mm^{-1})	0.940	1.298	0.930	1.069	1.052
F(0 0 0)	804	888	800	804	1032
Range of *h*, *k*, *l*	−9/9, −20/22, −13/14	−9/11, −14/14, −16/17	−17/16, −10/10, −10/16	−17/17, −5/10, −16/16	−10/10, −14/17, −19/20
Total/independent reflns	9566/5416	8654/1522	4169/1473	4277/1454	11336/3799
Parameters	505	123	124	124	282
R_{int}	0.0340	0.0209	0.0230	0.0176	0.0371
R^a, $R_w{}^b$	0.0553, 0.1286	0.0173, 0.0473	0.0289, 0.0640	0.0268, 0.0764	0.0422, 0.1131
GOF^c	1.072	1.047	1.138	1.036	1.065
Residuals (e Å^{-3})	0.574, −0.355	0.220, −0.382	0.217, −0.194	0.354, −0.237	0.895, −0.659

[a] $R = \Sigma||F_o|-|F_c||/\Sigma|F_o|$.
[b] $R_w = [\Sigma[w(F_o^2-F_c^2)^2]/\Sigma w(F_o^2)^2]^{1/2}$.
[c] $GOF = \{\Sigma[w(F_o^2-F_c^2)^2]/(n-p)\}^{1/2}$.

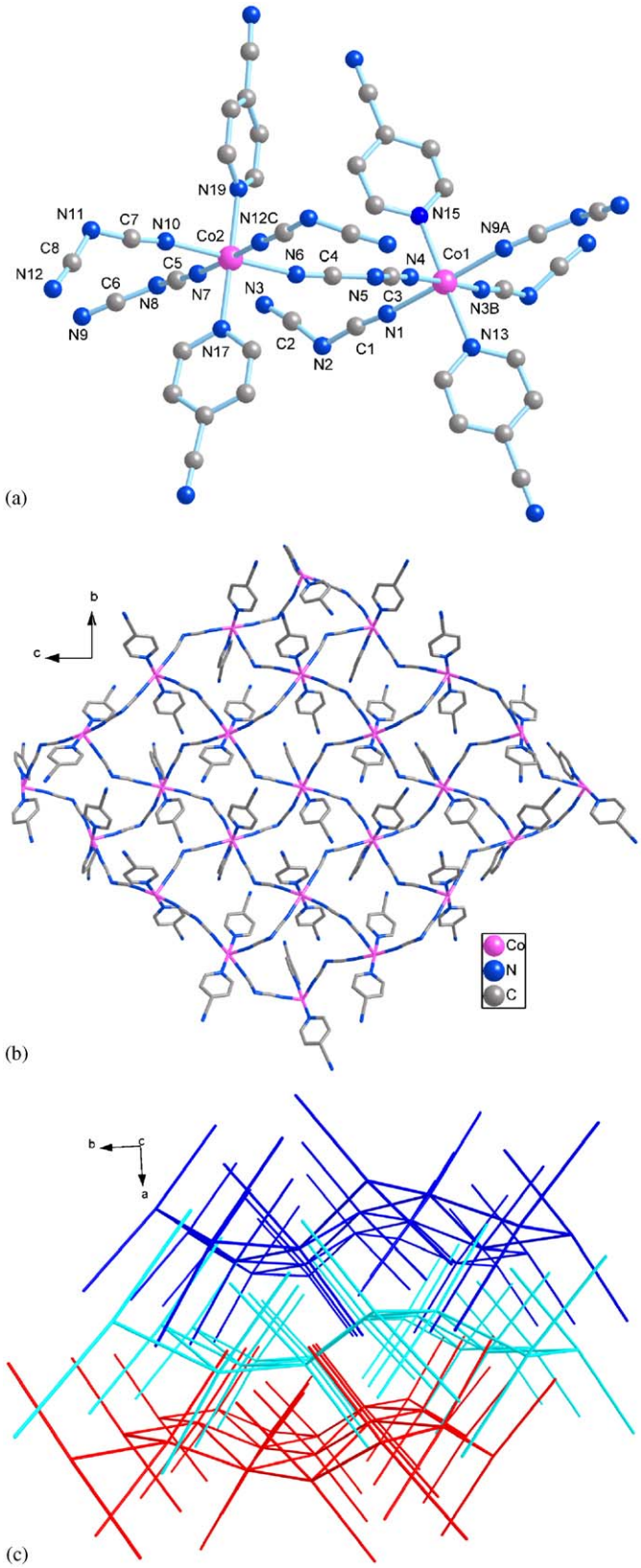

Fig. 1. (a) A portion view of **1** with atom labeling of metal coordination spheres and independent dca anions. (b) A perspective view of the 2-D coordination layer in **1**. (c) A schematic illustration of the interdigitated packing of the 2-D arrays in **1**.

(peak: 217 °C) may be attributed to the release of four 4-cypy ligands (calculated: 52.15%). The remaining substance retains intact until two consecutive steps of weight loss beyond 386 °C (peaks: 644 and 681 °C), which does not stop until heating to 800 °C. For complex **2**, two consecutive steps of weight loss occur in 112–311 °C (peaks: 188 and 280 °C), corresponding to the pyrolysis of two 4-cypy molecules (calculated/observed: 45.99/46.15%). Further heating to 800 °C suggests a continuous and slow weight loss. The TGA curve of **3** shows two consecutive weight losses of 52.75% in the range of 124–286 °C (peaks: 180 and 233 °C), indicating the expulsion of two 3-cypy ligands (calculated: 52.56%). Then it undergoes a slow weight loss of 28.58% that ends at 556 °C (peak: 356 °C). The TGA curve of **4** is quite similar to that of **1**. The first sharp weight loss of 52.88% in 138–218 °C (peak: 206 °C) indicates the release of 3-cypy (calculated: 52.15%). The residue starts to decompose at 281 °C with two consecutive weight losses (peaks: 647 and 682 °C) and does not end until heating to 800 °C.

3.2. Structural analysis of complexes *1–5*

3.2.1. $[Co_2(dca)_4(4\text{-cypy})_4]_n$ (*1*) and $[Cd(dca)_2(4\text{-cypy})_2]_n$ (*2*)

The crystal structures of **1** and **2** consist of 2-D metal–dca layers with lateral 4-cypy terminals, which however are different as described below. For **1**, two crystallographically independent Co^{II} centers are similarly six-coordinated to four equatorial dca nitrogen atoms and two axial *trans*-4-cypy ligands, showing a distorted octahedral geometry (Fig. 1a). Normally, the Co–N_{py} lengths are longer than those of Co–N_{dca} (see Table 2). Each dca anion takes the $\mu_{1,5}$-binding fashion with Co^{II} and as a consequence, the metal centers are interlinked by dca to produce a 2-D corrugated layer (Fig. 1b). Notably, there are two types of quadrangular units in this 2-D (4,4) network. One is composed of three Co1 and one Co2, while the other is three Co2 and one Co1. The adjacent Co⋯Co separations are 8.037(3) Å for Co1⋯Co1, 7.745(3) Å for Co2⋯Co2, and 8.35(2)/8.40(2) Å for Co1⋯Co2. These 2-D layers are parallel along the [100] direction. It is worth to highlight that due to the undulating character of the 2-D layer, a portion of the 4-cypy molecules in each layer penetrates into two adjacent 2-D arrays to give a cross-linked 3-D packing motif, as illustrated in Fig. 1c.

In the structure of **2**, the octahedral Cd^{II} center is also coordinated to four $\mu_{1,5}$-dca ligands via the nitrile nitrogens and two 4-cypy via the pyridyl nitrogen donors, which however adopts a *cis* arrangement in the coordination sphere (see Fig. 2a). Selected bond parameters for **2** are listed in Table 3, indicating the longer Cd–N_{py} lengths compared with those of Cd–N_{dca}. The dca anions connect the Cd^{II} centers via the end-to-end bridging mode to give a 2-D layer along (1 1 0) as shown in Fig. 2b. This (4,4) net has the dimensions of 8.407(1) Å along two directions, and the angles of the rhombus repeating unit are 95.41(1) and

Table 2
Selective bond lengths (Å) and angles (°) for complex **1**

Bond lengths			
Co1–N4	2.079(6)	Co1–N1	2.113(7)
Co1–N9A	2.120(7)	Co1–N3B	2.124(6)
Co1–N13	2.156(6)	Co1–N15	2.179(7)
Co2–N12C	2.066(6)	Co2–N10	2.119(6)
Co2–N6	2.122(6)	Co2–N7	2.139(6)
Co2–N19	2.149(6)	Co2–N17	2.181(6)
N1–C1	1.15(1)	N2–C1	1.29(1)
N2–C2	1.32(1)	N3–C2	1.135(9)
N4–C3	1.148(9)	N5–C4	1.29(1)
N5–C3	1.30(1)	N6–C4	1.145(9)
N7–C5	1.11(1)	N8–C6	1.31(1)
N8–C5	1.31(1)	N9–C6	1.11(1)
N10–C7	1.128(9)	N11–C7	1.32(1)
N11–C8	1.319(9)	N12–C8	1.167(9)
Bond angles			
N4–Co1–N1	90.1(3)	N4–Co1–N9A	93.8(3)
N1–Co1–N9A	175.7(3)	N4–Co1–N3B	177.9(3)
N1–Co1–N3B	89.7(3)	N9A–Co1–N3B	86.6(3)
N4–Co1–N13	89.9(2)	N1–Co1–N13	90.7(2)
N9A–Co1–N13	91.3(3)	N3B–Co1–N13	88.0(2)
N4–Co1–N15	92.8(3)	N1–Co1–N15	89.3(3)
N9A–Co1–N15	88.6(3)	N3B–Co1–N15	89.3(2)
N13–Co1–N15	177.3(2)	N12A–Co2–N10	89.3(3)
N12C–Co2–N6	90.3(2)	N10–Co2–N6	179.5(3)
N12C–Co2–N7	177.8(3)	N10–Co2–N7	88.5(3)
N6–Co2–N7	91.8(2)	N12C–Co2–N19	90.6(3)
N10–Co2–N19	89.5(2)	N6–Co2–N19	90.1(3)
N7–Co2–N19	89.1(2)	N12C–Co2–N17	90.4(2)
N10–Co2–N17	90.1(2)	N6–Co2–N17	90.3(2)
N7–Co2–N17	89.9(2)	N19–Co2–N17	178.9(2)

Symmetry codes: A $x, y, z+1$; B $x, -y+1, z+1/2$; C $x, -y, z+1/2$.

68.92(1)°. Investigation of the crystal packing shows that the pairs of *cis*-4-cypy segments, located up and down each 2-D array, insert into the side spaces of two adjacent parallel layers to form an interdigitated tactic motif (see Fig. 2c). Notably, **2** is isostructural to its Mn^{II} family $[Mn(dca)_2(4\text{-cypy})_2]_n$ [7e].

3.2.2. $[Fe(dca)_2(3\text{-cypy})_2]_n$ (**3**) and $[Co(dca)_2(3\text{-cypy})_2]_n$ (**4**)

Single-crystal X-ray diffraction results reveal that complexes **3** and **4** are isostructural with a general formula $[M(dca)_2(3\text{-cypy})_2]_n$. As depicted in Fig. 3a, the octahedral metal ion, lying on a point of symmetry center, is coordinated to four equatorial dca anions using their terminal nitrogen atoms and a pair of *trans*-3-cypy ligands occupying the axial sites. As expected, the M–N_{py} distances are longer than those of M–N_{dca} in each structure, and all Fe−N lengths are significantly longer than those of the corresponding Co–N bonds (see Table 4). Similarly, the $\mu_{1,5}$-dca anions again connect the metal centers to generate a 2-D rhombus layer (see Fig. 3b). The adjacent $M\cdots M$ distances within a layer are 8.251(3) Å for **3** and 8.194(1) Å for **4**. These 2-D (4,4) arrays are interdigitated to engender a regular 3-D lattice, which are interestingly managed by aromatic stacking between the parallel 3-cypy segments, as

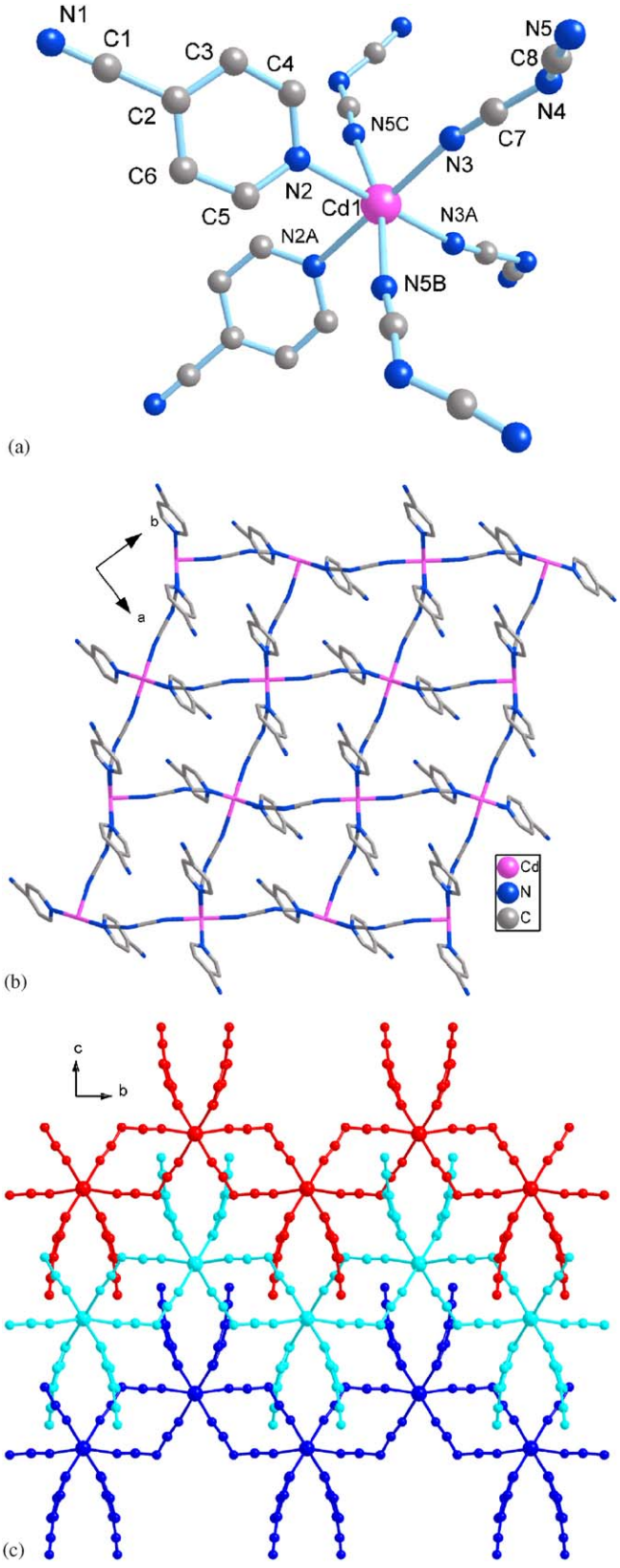

Fig. 2. (a) A portion view of **2** with atom labeling of the asymmetric unit and Cd^{II} coordination sphere. (b) A perspective view of the 2-D coordination layer in **2**. (c) The packing diagram of **2** showing the interdigitation of the 2-D layers.

Table 3
Selective bond lengths (Å) and angles (°) for complex **2**

Bond lengths			
Cd1–N3	2.286(2)	Cd1–N5B	2.308(2)
Cd1–N2	2.406(2)	N3–C7	1.148(3)
N4–C7	1.297(3)	N4–C8	1.299(3)
N5–C8	1.140(3)		
Bond angles			
N3–Cd1–N3A	92.7(1)	N3–Cd1–N5B	95.53(7)
N3A–Cd1–N5B	94.27(7)	N5B–Cd1–N5C	165.8(1)
N3–Cd1–N2	86.76(7)	N3A–Cd1–N2	178.86(6)
N5B–Cd1–N2	84.82(6)	N5C–Cd1–N2	85.50(6)
N2–Cd1–N2A	93.84(8)		

Symmetry codes: A $1/2-x$, $1/2-y$, z; B $x-1/2$, $-y$, $1/2-z$; C $1-x$, $y+1/2$, $1/2-z$.

shown in Fig. 3c. The centroid-to-face and centroid-to-centroid distances are 3.33 and 3.47 Å for **3**, and 3.56 and 3.65 Å for **4**, respectively.

3.2.3. *[Cd(dca)$_2$(pyom)$_2$] (**5**)*

Complex **5** is a discrete monomeric molecule as depicted in Fig. 4a, in which the in situ generation of the ligand *O*-methyl picolinimidate is validated by X-ray diffraction. Two pyom chelated ligands and a pair of monodentate dca terminals provide the local coordination environment of Cd^{II}, resulting in a distorted octahedron. As generally observed, the dca anions do not coordinate to the metal center linearly in **1–5**. As listed in Table 5, the Cd–N bond lengths follow a decreasing order for pyridyl, imine and nitrile donors, indicating the discrepancy of their coordination ability. Moreover, one free nitrile nitrogen of dca acts as the acceptor of the N1–H1···N7 [H···N/N···N lengths: 2.40/3.24 Å; angle: 167°; symmetry code: $-x$, $1-y$, $-z$] and N4–H1···N7 [H···N/N···N lengths: 2.35/3.20 Å; angle: 171°; symmetry code: $-x-1$, $-y+1$, $-z$] H-bonds with the imine groups from pyom. As a result, the complex molecules are linked by such secondary interactions to form a 1-D tape (Fig. 4b). Viewing along the [100] axis (see Fig. S1), the neighboring 1-D arrays are almost perpendicular and arrange alternately.

3.3. *Magnetic properties of complexes **1**, **3** and **4***

3.3.1. *Complexes **1** and **4***

An important experimental feature in almost all octahedral Co^{II} complexes is that the $\chi_M T$ (or μ_{eff}) values at r.t. are larger than those expected for the isolated spin-only ion ($\chi_M T = 1.87\,cm^3\,mol^{-1}\,K$ for a $S = 3/2$ ion), indicating that a significant orbital contribution is involved [13]. Typical values of $\chi_M T$ (or μ_{eff}) are 2.75–3.40 $cm^3\,mol^{-1}\,K$ (4.7–5.2 μ_β) [13,14], and lower values indicate a perturbation from the ideal octahedral geometry [14]. For complex **1**, the $\chi_M T$ vs. T plot (χ_M is the molar magnetic susceptibility for one Co^{II} ion) is shown in Fig. 5a. The $\chi_M T$ value at 300 K is 3.4 $cm^3\,mol^{-1}\,K$ and

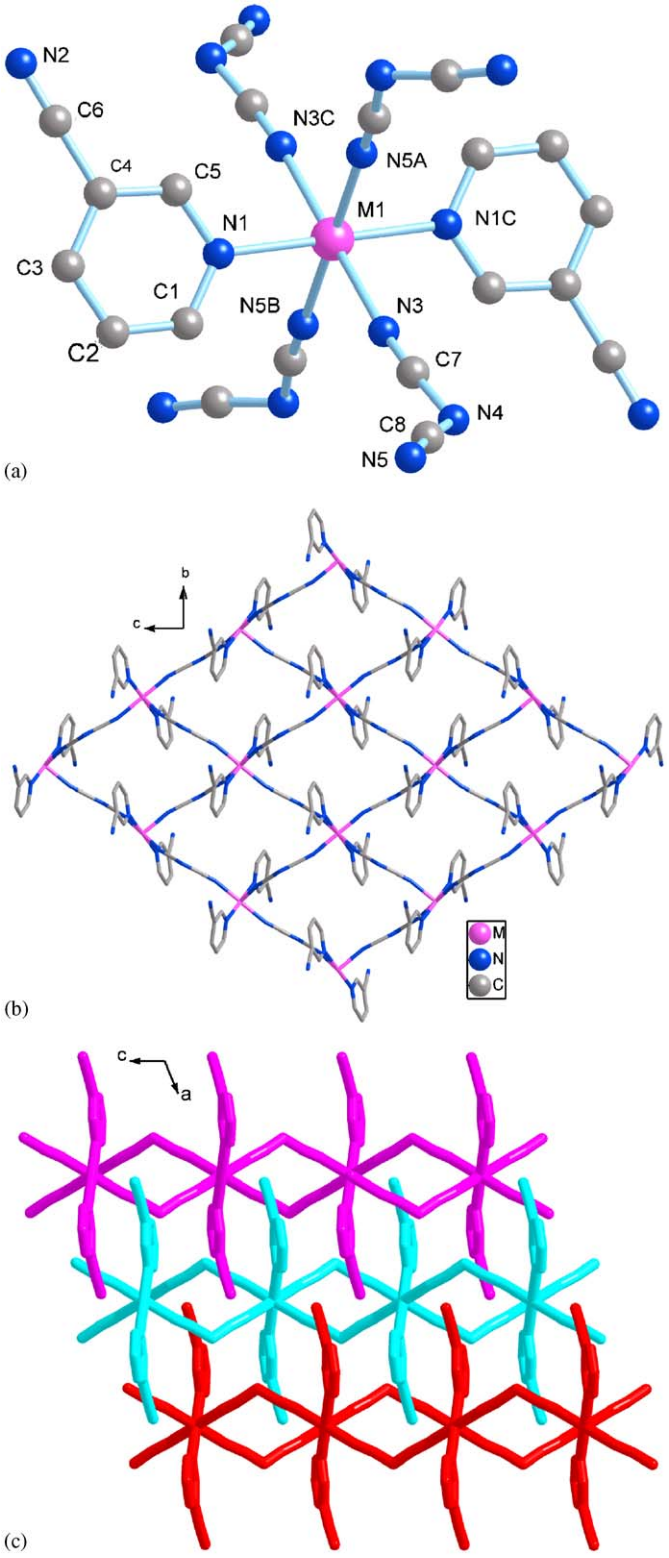

Fig. 3. (a) A portion view of **3/4** with atom labeling of the asymmetric unit and metal coordination sphere. (b) A perspective view of the 2-D coordination layer in **3/4**. (c) The packing diagram of **3/4** showing the interdigitation of the 2-D layers.

continuously decreases to 1.8 $cm^3\,mol^{-1}\,K$ at 2 K. At lower temperatures (from 15 to 2 K) there are significant differences in the $\chi_M T$ values applying small magnetic

Table 4
Selective bond lengths (Å) and angles (°) for complexes **3** and **4**

	3	**4**
M1–N5A	2.159(2)	2.126(2)
M1–N3	2.170(2)	2.125(2)
M1–N1	2.198(2)	2.147(2)
N3–C7	1.152(3)	1.150(3)
N4–C7	1.310(3)	1.311(3)
N4–C8	1.311(3)	1.311(3)
N5–C8	1.149(3)	1.155(3)
N3–M1–N5A	90.21(8)	90.11(7)
N3–M1–N5B	89.79(8)	89.89(7)
N3C–M1–N1	89.62(8)	92.46(7)
N3–M1–N1	90.38(8)	87.54(7)
N5A–M1–N1	87.15(7)	90.80(7)
N5B–M1–N1	92.85(7)	89.20(7)

Symmetry codes: (**3**) A $1/2-x$, $y-1/2$, $1/2-z$; B x, $1-y$, $z-1/2$; C $1/2-x$, $1/2-y$, $-z$. (**4**) A $1/2-x$, $y+1/2$, $1/2-z$; B x, $1-y$, $z-1/2$; C $1/2-x$, $3/2-y$, $-z$.

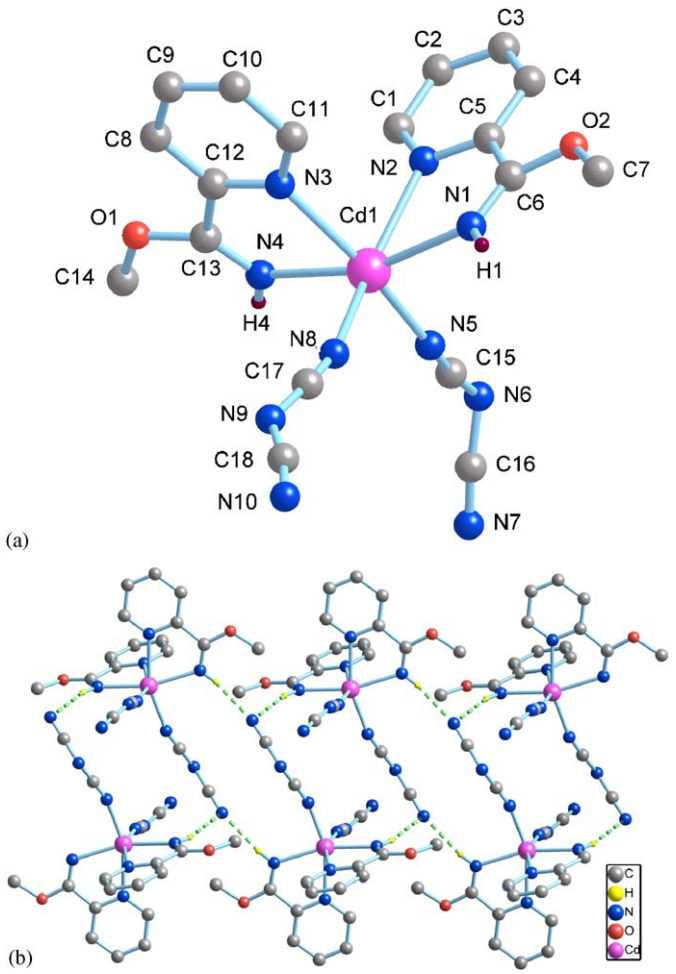

Fig. 4. (a) The molecular structure of complex **5** with atom labeling (irrelevant H atoms are omitted for clarity). (b) 1-D hydrogen-bonded motif of **5**.

fields, indicating the presence of a small amount of ferromagnetic or canted antiferromagnetic-ordered impurities, likely α- or β-$[Co(dca)_2]_n$, with T_c at 9–10 K [3,15].

Table 5
Selective bond lengths (Å) and angles (°) for complex **5**

Bond lengths			
Cd1–N8	2.259(5)	Cd1–N5	2.263(6)
Cd1–N1	2.313(5)	Cd1–N4	2.323(4)
Cd1–N3	2.353(4)	Cd1–N2	2.430(4)
O1–C13	1.327(7)	O1–C14	1.42(1)
N4–C13	1.239(7)	O2–C6	1.339(7)
O2–C7	1.40(1)	N1–C6	1.223(8)
N8–C17	1.112(8)	N9–C18	1.15(1)
N9–C17	1.27(1)	N10–C18	1.053(8)
N5–C15	1.117(7)	N6–C15	1.276(9)
N6–C16	1.31(1)	N7–C16	1.11(1)
Bond angles			
N8–Cd1–N5	102.2(2)	N8–Cd1–N1	93.8(2)
N5–Cd1–N1	99.4(2)	N8–Cd1–N4	98.6(2)
N5–Cd1–N4	90.5(2)	N1–Cd1–N4	162.2(2)
N8–Cd1–N3	89.2(2)	N5–Cd1–N3	159.5(2)
N1–Cd1–N3	96.8(2)	N4–Cd1–N3	70.9(2)
N8–Cd1–N2	161.3(2)	N5–Cd1–N2	89.0(2)
N1–Cd1–N2	69.4(2)	N4–Cd1–N2	96.2(2)
N3–Cd1–N2	84.9(2)		

This feature is, unfortunately, very frequent in most of the Co^{II}–dca–L derivatives [5,16].

It is similar in the case of **4** (see Fig. 5b), with $\chi_M T$ value at 300 K being 3.5 $cm^3\,mol^{-1}\,K$. The $\chi_M T$ values continuously decrease to 2.2 $cm^3\,mol^{-1}\,K$ at 12 K. Also, significant differences in $\chi_M T$ values applying small magnetic fields were observed from 12 to 2 K. To be sure of the presence of the impurities as stated above, ac susceptibility measurement was made for **4** (see Fig. S2). The T_c is ~9 K, being consistent with that for $[Co(dca)_2]_n$. The reduced magnetization curve, $M/N\beta$, at 2 K tends to 2.3 or 2.5 $N\beta$ for **1** or **4** at 2 T (Fig. 5 inset), being a typical value for distorted octahedral Co^{II} complexes.

Considering the spin–orbit coupling due to the $^4T_{1g}$ ground state for octahedral Co^{II} complexes [13], exact calculations for deriving the J parameter from experimental data in all the temperature range is impossible unless for the dinuclear complexes [17]. Other small polynuclear systems can also be fitted through sophisticated computer programs at low-temperature region (where the effective spin S' is $\frac{1}{2}$), based on full diagonalization methods [18]. 1-D systems of Co^{II} are frequently associated with anisotropic Ising systems, and they can be fitted in the low-temperature zone assuming again an effective spin $S' = \frac{1}{2}$ [19]. To date it is impossible to fit the high-temperature region of 1-D or 2-D Co^{II} complexes owing to the existence of λ (spin–orbit coupling), A (measure of the strength of the crystal field), distortion respect to the regular octahedral geometry and J. The only possibility is trying to calculate an estimated J value using the two-exponential Rueff expression, which is suitable for any temperature greater than the possible T_c. In fact, Rueff et al. [19c,20] have proposed a phenomenological approach for some low-dimensional Co^{II} systems that allows to have

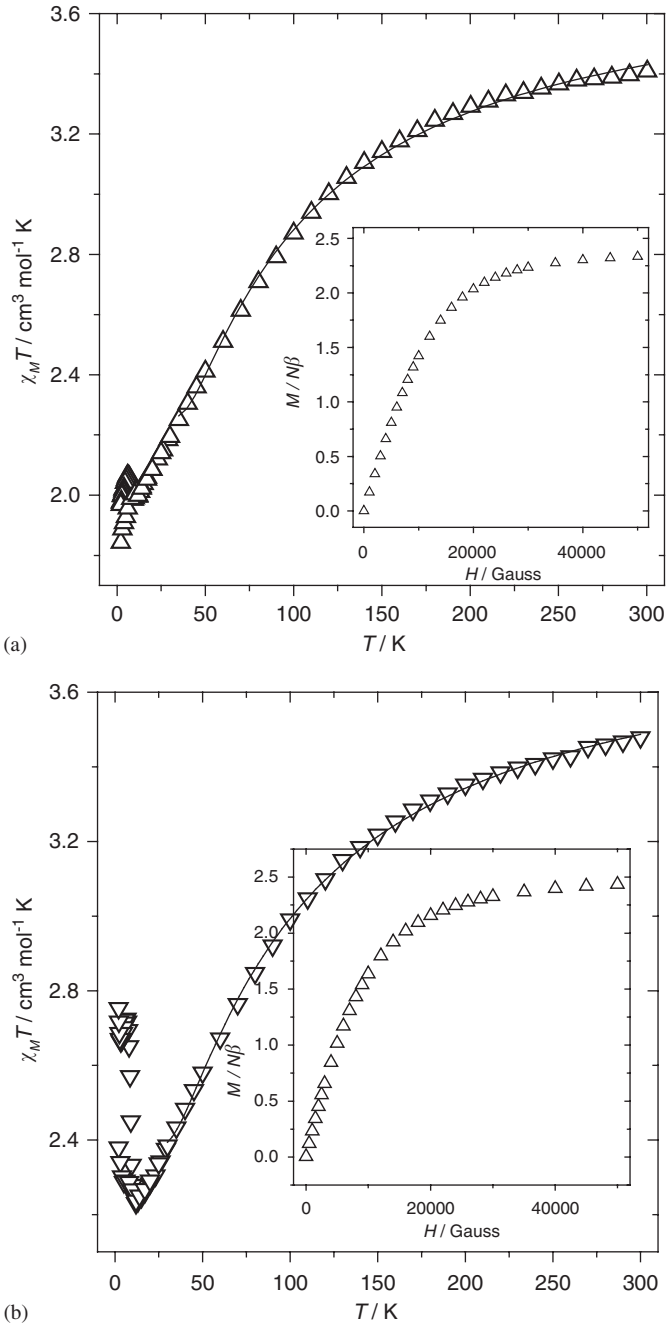

Fig. 5. (a) Plot of the $\chi_M T$ vs. T for complex **1**. (b) Plot of the $\chi_M T$ vs. T for complex **4**. Solid line from r.t. to 30 K represents the best fit with the formula of Rueff. Inset: Plot of the reduced magnetization at 2 K.

an *estimate* of the strength of the antiferromagnetic exchange interactions. They postulate the phenomenological equation:

$$\chi_M T = A\,\exp(-E_1/kT) + B\,\exp(-E_2/kT)$$

in which, $A+B$ equals the Curie constant ($\approx$2.8–3.4 cm^3 mol^{-1} K for octahedral Co^{II} ions), and E_1, E_2 represent the "activation energies" corresponding to the spin–orbit coupling and the antiferromagnetic exchange interaction. E_1/k, the effect of spin–orbit coupling and site distortion is of the order of $+100$ K [19c,20,21]. This equation adequately describes the spin–orbit coupling, resulting in a splitting between the discrete levels, and the exponential low-temperature divergence of the susceptibility. Very good results have been obtained for some 1-D and 2-D Co^{II} complexes [19c,20].

The fit values obtained with this procedure for **1** and **4** (from $\chi_M T$ curves with $H = 1$ T; from 300 to 25 K to avoid the effect of the magnetic ordering at low temperatures) are $A+B = 3.12$ and 3.33 cm^3 mol^{-1} K, respectively, which agrees well with those given in the literatures for the Curie constant [19c,20]. $E_1/k = 71.2$ K (for **1**) and 54.3 K (for **4**) are of the same magnitude compared with those reported by Rueff et al. for several 1-D and 2-D Co^{II} systems [20]. As for the value found for the antiferromagnetic exchange interaction, it is very weak ($E_2/k = 0.57$ and 0.85 K), corresponding to $J = -1.14$ and -1.7 K (-0.80 and -1.18 cm^{-1}) according to the Ising chain approximation, $\chi_M T \propto \exp(J/2kT)$. The small J value is compatible with the $\mu_{1,5}$-dca bridge, which always gives almost negligible coupling parameters [13b].

3.3.2. Complex 3

3.3.2.1. Magnetic consideration about Fe^{II} ion. In the octahedral ligand field, the free ion ground term ^{5}D of the d^6 configuration splits into $^5T_{2g}$ and ^5E_g terms, the former lying ca. 10.000 cm^{-1} below the latter. The $^5T_{2g}$ ground term has the first-order spin–orbit coupling. The expression of χ_M vs. T including λ (-103 cm^{-1} for the free ion) can be found in several books [22]. At room temperature a $\chi_M T$ value of ca. 4.0 cm^3 mol^{-1} K is expected, which should remain nearly independent of temperature in the liquid nitrogen temperature range. However, the experimental magnetic moments are usually less than this expected value [22]. This is interpreted as a result of the departure from octahedral symmetry and/or electron delocalization. In the presence of the very frequent axial distortion, the splitting of the $^5T_{2g}$ term gives the $^5B_2$ and ^5E levels. Indeed, as indicated by Carlin [21], the problem with this $S = 2$ ion lies especially with the large number of electronic states. Being a non-Kramers ion, currently it has a large zero-field splitting (ZFS). For example, D has been reported [21] as 20 cm^{-1} and g-values deviate from 2.00. This consideration of the presence of strong ZFS, has allowed to treating most of the polynuclear Fe^{II} complexes as coming from ions without the first-order spin–orbit coupling but with a noticeable D value [23]. Lippard et al. have stated, for example, that significant ZFS for high-spin Fe^{II} makes it difficult to fit the magnetic data, especially when the ZFS effect is of the same magnitude as the exchange coupling interaction [23b,24].

Thus, many authors fit the experimental results for polynuclear Fe^{II} complexes assuming the spin-only equation for the effective moment of n independent $S = 2$ Fe^{II} ions, neglecting the ZFS at relatively high temperatures, with very good results. This indicates that, effectively, the first-order spin–orbit coupling is quenched [25]. In a similar

manner, 1-D systems, are usually fit applying the $S = 2$ Fisher formula [26] at not too low temperatures considering an isotropic Heisenberg model and neglecting the ZFS effect [27]. Unfortunately, the accurate fit of 2-D Fe^{II} systems, such as complex **3**, is impossible.

3.3.2.2. Magnetic data for complex 3. The shape of the $\chi_M T$ vs. T curve for **3** is given in Fig. 6a, starting at $4.08\,cm^3\,mol^{-1}\,K$ approximately (close to the upper limit assuming spin–orbit coupling). From room temperature to 70 K the $\chi_M T$ values are almost constant and then decrease rapidly to $3.7\,cm^3\,mol^{-1}\,K$ at 18 K. From 18 to 2 K there is an increasing to $3.8\,cm^3\,mol^{-1}\,K$ and a final sharp decreasing to $3.42\,cm^3\,mol^{-1}\,K$ at 2 K. The final low-temperature region is field-dependent. The high-temperature region is typical for a Fe^{II} case with a small antiferromagnetic coupling. The low-temperature region (susceptibility-dependence of the field) could be a signal of long-range order, likely due to a small amount of impurities of $[Fe(dca)_2]_n$, which is a canted spin antiferromagnet [3].

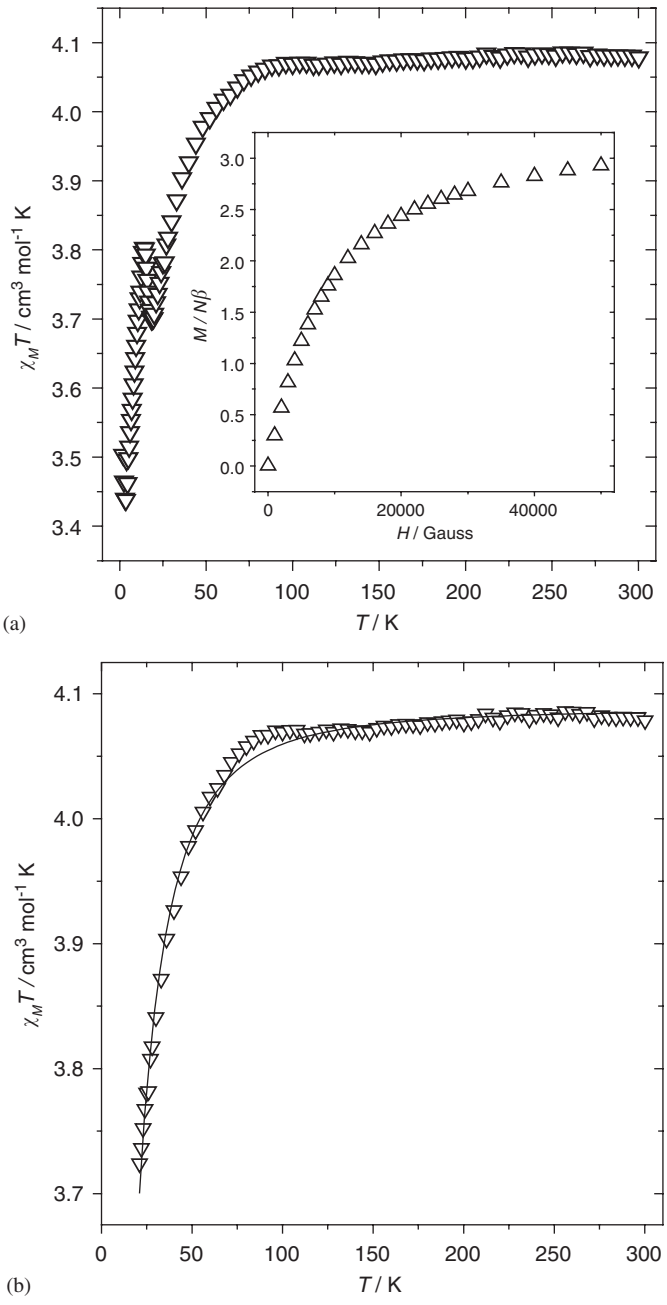

Fig. 6. (a) Plot of the $\chi_M T$ **vs.** T for **3**. Inset: Plot of the reduced magnetization at 2 K. (b) Plot of the high-temperature region of $\chi_M T$ vs. T for **3**. Solid line represents the fit made assuming an isolated Fe^{II} with zero-field splitting (D parameter).

The $\chi_M T$ curve ($H = 1$ T; from 300 to 25 K to avoid the effect of the magnetic ordering at low temperatures) may be fit assuming the ZFS parameter D in a non-coupled Fe^{II} ion. The fit was obtained applying the formula given by Edwards et al. [28] and gave the following values: $D = -2.45\,cm^{-1}$ and $g = 2.33$ (Fig. 6b). The g value is excess of 2.00 as a result of the spin–orbit coupling in the $^5T_{2g}$ electronic state, and the value of D is well within the range expected for six-coordinated high-spin Fe^{II} complexes [21]. Anyway, J value should be very small as predicted for $\mu_{1,5}$-dca bridging ligand (see below). The plot of the reduced magnetization ($M/N\beta$) vs. H at 2 K is a typical plot for a quasi-isolated Fe^{II} ion (see Fig. 6a inset).

3.3.2.3. Dicyanamide as bridging ligand. In a recent review, a comprehensive study of the structural and magnetic data of coordination polymers containing dca bridging ligand has been reported [3]. From this review and references therein, a classification of these compounds is given. For example, the most important series (from magnetic point of view) is the rutile-like $[M(dca)_2]_n$ complexes ($M = V^{II}$, Cr^{II}, Mn^{II}, Fe^{II}, Co^{II}, Ni^{II}) which show magnetic ordering. They are ferromagnets for $M = Co^{II}$ and Ni^{II} below 9 and 21 K, and weak (canted) antiferromagnets for $M = Cr^{II}$, Mn^{II}, and Fe^{II}, below 47, 16 and 18 K, respectively. Significantly, tridentate $\mu_{1,3,5}$-dca is presented in all these structures, allowing access to M–NCN–M magnetic exchange pathways. In contrast, when there is an ancillary ligand L (being Lewis bases such as pyridine, dipyridine, pyrazine, 4-cyanopyridine and 1,2-bis(4-pyridyl)ethane) and only bidentate $\mu_{1,5}$-dca is present, long-range ordering is usually not observed [3]. In these cases the coupling is almost exclusively antiferromagnetic and weak, and the ferromagnetic coupling in polynuclear complexes with $\mu_{1,5}$-dca is very rare [7b,8f,29]. Focusing our interest in Fe^{II} complexes, the number of them with magnetic studies is quite limited compared to those reported for other metal ions such as Cu^{II} and Mn^{II}. The parent complex $[Fe(dca)_2]_n$ is a canted antiferromagnet [2b,3]. Another weak ferromagnet (canted antiferromagnet) $[Fe(dca)_2(pyrimidine)]_n$ has been reported, which is very interesting as a comparison to **3**. It is a 3-D net formed by the linkage of Fe–dca layers via pyrimidine [30], which, with only $\mu_{1,5}$-dca bridges, displays weak ferromagnetism with an average T_c close to 5 K. Other similar 3-D nets, with different co-ligands such as pyrazine do not show ferromagnetic ordering [31]. To the best of our knowledge,

only one 2-D Fe–dca species $\{[Fe(dca)_2(4,4'\text{-bipy})]\cdot bt\}_n$ ($bt = 2,2$-bithiazoline) has been documented so far but *without* magnetic study [32]. Some 1-D systems have also been reported but without any magnetic ordering [27a,33]. Considering these data, we propose that the canted antiferromagnetism (weak ferromagnetism at low-temperature) in **3** is not intrinsic but corresponds to a very small amount of $[Fe(dca)_2]_n$ impurities. Indeed, the T_c of $[Fe(dca)_2]_n$ and **3** ($\sim$17 K) is practically the same (Fig. S3). Furthermore, the 3-D complex $[Fe(dca)_2(pyrimidine)]_n$ commented above shows a T_c of only 5 K [30]. It seems very unlikely that a similar 2-D complex can show a larger T_c, such as in **3**.

The presence of $[M(dca)_2]_n$ impurities in $[M(dca)_2L]_n$ complexes has already been noticed in some similar cases. At this respect, it can be useful to underline a statement given by Murray and coworkers in their work on $(Ph_4As)[Ni(dca)_3]$: "… great care (is) required to make sure that traces of contaminants are eliminated or minimized, even in systems that are crystalline and structurally characterized. This is important in systems that can give magnetically ordered contaminants as byproducts." [34]. Unfortunately, an amount of less than 0.1% of a ferromagnet impurity, will give the typical features at low temperature, mainly when $\chi_M T$ tends to zero.

4. Conclusion

In this research, we describe four Fe^{II}, Co^{II}, and Cd^{II} layered polymers via $\mu_{1,5}$-dca anions with the monodentate cypy auxiliary ligands. Interestingly, their Cu^{II} analogues have distinct chain structures via double $\mu_{1,5}$-dca bridges though the metal centers have a similar octahedral sphere ($4_{dca}+2_{cypy}$) in all these complexes, indicating a subtle role of metal ions in this system. The magnetic coupling in **1**, **3** and **4** is antiferromagnetic and very weak, which is as expected considering the end-to-end bridging mode of dca. However, the $\chi_M T$ values are field-dependent at low-temperature region for all three cases, which should be ascribed to the existence of trace impurities of $[M(dca)_2]_n$ ($M = Co^{II}$ or Fe^{II}) that is commonly observed in the *M*–dca–L systems. As for **3**, the present work represents the first magnetic study for a 2-D Fe–dca complex, which is also very rare from the structural viewpoint.

Acknowledgments

This work was financially supported by the National Natural Science Foundation of China (No. 20401012), the Key Project of Chinese Ministry of Education (No. 205008), the National Fundamental Research Project of China (No. 2005CCA01200) and the Spanish Government (No. BQU2003/00539).

Appendix A. Supplementary material

Crystallographic data for the crystal structures reported in this paper have been deposited with the Cambridge Crystallographic Data Center (CCDC Nos. 604681–604685). This material can be obtained free of charge via www.ccdc.cam.ac.uk/conts/retrieving.html.

Supplementary data associated with this article can be found, in the online version, at doi:10.1016/j.jssc.2006.08.0.39.

References

[1] (a) B. Moulton, M.J. Zaworotko, Chem. Rev. 101 (2001) 1629;
(b) C. Janiak, Dalton Trans. (2003) 2781.
[2] (a) S.R. Batten, P. Jensen, B. Moubaraki, K.S. Murray, R. Robson, Chem. Commun. (1998) 439;
(b) M. Kurmoo, C.J. Kepert, New J. Chem. 22 (1998) 1515.
[3] A nice review on coordination chemistry of dca is described in S.R. Batten, K.S. Murray, Coord. Chem. Rev. 246 (2003) 103.
[4] (a) J.P. Costes, G. Novitchi, S. Shova, F. Dahan, B. Donnadieu, P. Tuchagues, Inorg. Chem. 43 (2004) 7792;
(b) A.M. Madalan, C. Paraschiv, J.P. Sutter, M. Schmidtmann, A. Müller, M. Andruh, Cryst. Growth Des. 5 (2005) 707;
(c) D. Ghoshal, A.K. Ghosh, J. Ribas, E. Zangrando, G. Mostafa, T.K. Maji, N.R. Chaudhuri, Cryst. Growth Des. 5 (2005) 941;
(d) H.L. Sun, B.Q. Ma, S. Gao, S.R. Batten, Cryst. Growth Des. 5 (2005) 1331;
(e) H. Miyasaka, K. Nakata, L. Lecren, C. Coulon, Y. Nakazawa, T. Fujisaki, K. Sugiura, M. Yamashita, R. Clerac, J. Am. Chem. Soc. 128 (2006) 3770.
[5] A.M. Kutasi, A.R. Harris, S.R. Batten, B. Moubaraki, K.S. Murray, Cryst. Growth Des. 4 (2004) 605.
[6] (a) W. Dong, Q.-L. Wang, Z.-Q. Liu, D.-Z. Liao, Z.-H. Jiang, S.-P. Yan, P. Cheng, Polyhedron 22 (2003) 3315;
(b) J. Carranza, J. Sletten, F. Lloret, M. Julve, Inorg. Chim. Acta 357 (2004) 3304;
(c) R. Boca, M. Boca, M. Gembicky, L. Jager, C. Wagner, H. Fuess, Polyhedron 23 (2004) 2337;
(d) R. Karmakar, C.R. Choudhury, D.L. Hughes, G.P.A. Yap, M.S. El Fallah, C. Desplanches, J.P. Sutter, S. Mitra, Inorg. Chim. Acta 359 (2006) 1184.
[7] (a) S.R. Batten, P. Jensen, C.J. Kepert, M. Kurmoo, B. Moubaraki, K.S. Murray, D.J. Price, J. Chem. Soc. Dalton Trans. (1999) 2987;
(b) A. Escuer, F.A. Mautner, N. Sanz, R. Vicente, Inorg. Chem. 39 (2000) 1668;
(c) J.L. Manson, A.M. Arif, C.D. Incarvito, L.M. Liable-Sands, A.L. Rheingold, J.S. Miller, J. Solid State Chem. 145 (1999) 369;
(d) G.A. van Albada, M.E. Quiroz-Castro, I. Mutikainen, U. Turpeinen, J. Reedijk, Inorg. Chim. Acta 298 (2000) 221;
(e) S. Dalai, P.S. Mukherjee, E. Zangrando, N.R. Chaudhuri, New J. Chem. 26 (2002) 1185.
[8] (a) I. Dasna, S. Golhen, L. Ouahad, M. Fettouhi, O. Pena, N. Daro, J.P. Sutter, Inorg. Chim. Acta 326 (2001) 37;
(b) I. Dasna, S. Golhen, L. Ouahab, N. Daro, J.P. Sutter, New J. Chem. 25 (2001) 1572;
(c) G.A. van Albad, I. Mutikainen, U. Turpeinen, J. Reedijk, Acta Crystallogr. E 57 (2001) 421;
(d) J. Carranza, C. Brennan, J. Sletten, F. Lloret, M. Julve, J. Chem. Soc. Dalton Trans. (2002) 3164;
(e) J.-H. Luo, M.-C. Hong, J.-B. Weng, Y.-J. Zhao, R. Cao, Inorg. Chim. Acta 329 (2002) 59;

(f) B. Vangdal, J. Carranza, F. Lloret, M. Julve, J. Sletten, J. Chem. Soc. Dalton Trans. (2002) 566.
[9] Z.-M. Wang, B.-W. Sun, J. Luo, S. Gao, C.-S. Liao, C.-H. Yan, Y. Li, Inorg. Chim. Acta 332 (2002) 127.
[10] M. Du, X.-J. Zhao, S.R. Batten, J. Ribas, Cryst. Growth Des. 5 (2005) 901.
[11] (a) D. Venkataraman, S. Lee, J.S. Moore, P. Zhang, K.A. Hirsch, G.B. Gardner, A.C. Covey, C.L. Prentice, Chem. Mater. 8 (1996) 2030;
(b) K.A. Hirsch, S.R. Wilson, J.S. Moore, Inorg. Chem. 36 (1997) 2960;
(c) H.P. Wu, C. Janiak, G. Rheinwald, H. Lang, J. Chem. Soc. Dalton Trans. (1999) 183.
[12] (a) Bruker AXS, SAINT Software Reference Manual, Madison, WI, 1998;
(b) G.M. Sheldrick, SHELXTL NT Version 5.1. Program for Solution and Refinement of Crystal Structures, University of Göttingen, Germany, 1997.
[13] (a) F.E. Mabbs, D.J. Machin, Magnetism and Transition Metal Complexes, London, 1973;
(b) J.W. Raebiger, J.L. Manson, R.D. Sommer, U. Geiser, A.L. Rheingold, J.S. Miller, Inorg. Chem. 40 (2001) 2578;
(c) E.W. Lee, Y.J. Kim, D.Y. Jung, Inorg. Chem. 41 (2002) 501;
(d) B.N. Figgis, M.A. Hitchman, Ligand Field Theory and Its Applications, Wiley-VCH, New York, 2000;
(e) D. Armentano, G. De Munno, F. Lloret, M. Julve, Inorg. Chem. 38 (1999) 3744;
(f) S.J. Retting, R.C. Thompson, J. Trotter, S. Xia, Inorg. Chem. 38 (1999) 1360.
[14] (a) L.L. Lohr, J.C. Miller, R.R. Sharp, J. Chem. Phys. 111 (1999) 10148;
(b) S.G. Telfer, T. Sato, R. Kuroda, J. Lefebvre, D.B. Leznoff, Inorg. Chem. 43 (2004) 421.
[15] J.S. Miller, J.L. Manson, Acc. Chem. Res. 34 (2001) 563.
[16] (a) E. Colacio, F. Lloret, I.B. Maimoun, R. Kivekas, R. Sillanpaa, J. Suárez-Varela, Inorg. Chem. 42 (2003) 2720;
(b) P.M. van der Werff, S.R. Batten, P. Jensen, B. Moubaraki, K.S. Murray, J.D. Cashion, Cryst. Growth Des. 4 (2004) 503.
[17] (a) G. de Munno, M. Julve, F. Lloret, J. Faus, A. Caneschi, J. Chem. Soc. Dalton Trans. (1994) 1175;
(b) M.E. Lines, J. Chem. Phys. 55 (1971) 2977.
[18] (a) J.J. Borrás-Almenar, J.M. Clemente-Juan, E. Coronado, B.S. Tsukerblat, Inorg. Chem. 38 (1999) 6081;
(b) J.J. Borrás-Almenar, J.M. Clemente-Juan, E. Coronado, B.S. Tsukerblat, J. Comput. Chem. 22 (2001) 985.
[19] (a) M.E. Fisher, J. Math. Phys. 4 (1963) 124;
(b) S. Angelow, M. Drillon, E. Zhecheva, R. Stoyanova, M. Belaiche, A. Derory, A. Herr, Inorg. Chem. 31 (1992) 1514;
(c) J.-M. Rueff, N. Masciocchi, P. Rabu, A. Sironi, A. Skoulios, Eur. J. Inorg. Chem. (2001) 2843.
[20] J.-M. Rueff, N. Masciocchi, P. Rabu, A. Sironi, A. Skoulios, Chem. Eur. J. 8 (2002) 1813 and references therein.
[21] R.L. Carlin, Magnetochemistry, Springer, Berlin, 1986.
[22] See for example A.T. Casey, S. Mitra, in: E.A. Boudreaux, L.N. Mulay (Eds.), Theory and Applications of Molecular Parmagnetism, Wiley, New York, 1976 Chapter 3.
[23] (a) J.M. Clemente-Juan, C. Mackiewicz, M. Verelst, F. Dahan, A. Bousseksou, Y. Sanakis, J.-P. Tuchagues, Inorg. Chem. 41 (2002) 1478;
(b) D.P. Goldberg, J. Telser, C.M. Bastos, S.J. Lippard, Inorg. Chem. 34 (1995) 3011.
[24] R.C. Reem, E.I. Solomon, J. Am. Chem. Soc. 109 (1987) 1216.
[25] S. Herold, S.J. Lippard, Inorg. Chem. 36 (1997) 50 and references therein.
[26] M.E. Fisher, Am. J. Phys. 32 (1964) 343.
[27] (a) S. Martin, M.G. Barandika, J.M. Ezpeleta, R. Cortés, J.I.R. de Larramendi, L. Lezama, T. Rojo, J. Chem. Soc. Dalton Trans. (2002) 4275 and references therein;
(b) X. Hao, Y. Wei, S. Zhang, Chem. Commun. (2000) 2271.
[28] P.R. Edwards, C.E. Johnson, R.J.P. Williams, J. Chem. Phys. 47 (1967) 2074.
[29] D. Ghoshal, H. Bialas, A. Escuer, M. Font-Bardía, T.K. Maji, J. Ribas, X. Solans, R. Vicente, E. Zangrando, N.R. Chaudhuri, Eur. J. Inorg. Chem. (2003) 3929.
[30] (a) T. Kusaka, T. Ishida, D. Hashizume, F. Iwasaki, T. Nogami, Chem. Lett. (2000) 1146;
(b) N. Takagami, T. Ishida, T. Nogami, Bull. Chem. Soc. Jpn. 77 (2004) 1125.
[31] (a) P. Jensen, S.R. Batten, B. Moubaraki, K.S. Murray, J. Chem. Soc. Dalton Trans. (2002) 3713;
(b) P. Jensen, S.R. Batten, B. Moubaraki, K.S. Murray, J. Solid State Chem. 159 (2001) 352.
[32] A.B. Gaspar, M.C. Munoz, J.A. Real, Inorg. Chem. Commun. 7 (2004) 815.
[33] (a) J.L. Manson, A.M. Arif, J.S. Miller, J. Mater. Chem. 9 (1999) 979;
(b) S.R. Marshall, C.D. Incarvito, J.L. Manson, A.L. Rheingold, J.S. Miller, Inorg. Chem. 39 (2000) 1969.
[34] P.M. van der Werff, S.R. Batten, P. Jensen, B. Moubaraki, K.S. Murray, E.H.-K. Tan, Polyhedron 20 (2001) 1129.